



A Basic Study on the Performance of Tuned Dynamic Mass System Using Viscoelastic Damper

C. Kuo⁽¹⁾, I. Hata⁽²⁾, Y. Miyajima⁽³⁾, J. Mikami⁽⁴⁾, M. Ota⁽⁵⁾, K. Hirano⁽⁶⁾, K. Kato⁽⁷⁾,
N. Akuto⁽⁸⁾, T. Ichikawa⁽⁹⁾, Y. Kawaguchi⁽¹⁰⁾

⁽¹⁾ *i2S2.Co., Ltd., kaku@i2s2.co.jp*

⁽²⁾ *Professor, Dr. Eng., College of Science and Technology, Nihon University, hata.ipppei@nihon-u.ac.jp*

⁽³⁾ *President and CEO, i2S2. Co., Ltd., miyajima@i2s2.co.jp*

⁽⁴⁾ *i2S2.Co., Ltd., mikami@i2s2.co.jp*

⁽⁵⁾ *Bridgestone. Co., Ltd., masami.oota1@bridgestone.com*

⁽⁶⁾ *Bridgestone. Co., Ltd., kenji.hirano@bridgestone.com*

⁽⁷⁾ *Bridgestone. Co., Ltd., kouji.katou1@bridgestone.com*

⁽⁸⁾ *Graduate School of Science and Technology, Nihon University, csno18001@g.nihon-u.ac.jp*

⁽⁹⁾ *Graduate School of Science and Technology, Nihon University, csta19004@g.nihon-u.ac.jp*

⁽¹⁰⁾ *Graduate School of Science and Technology, Nihon University, csyk19017@g.nihon-u.ac.jp*

Abstract

In the wake of major earthquakes such as the 1995 Hyogo-ken Nanbu Earthquake and the 2011 off the Pacific coast of Tohoku Earthquake, it becomes very important how to design response control structures. In many cases, dampers are used as countermeasures against long-period ground motion in high-rise buildings. In high-rise buildings, the natural period of the 1st mode is long, so they are used to reduce the displacement response. On the other hand, in ground motions with short-period components such as inland earthquakes, the resonance phenomenon of the 2nd and 3rd modes greatly affect the acceleration response of high-rise buildings.

For example, if oil dampers (viscous dampers) are used in all layers as damping devices for high-rise buildings, they have the effect of giving viscous damping even in the 1st mode or second mode. However, a large number of dampers are required to give a large viscous damping. As an improvement method, the tuned dynamic mass system in which a viscous damper and a dynamic mass (D.M.) are arranged in parallel has been proposed.

The tuned dynamic mass system can give a large viscous damping with a small damping coefficient by the optimum design based on fixed point theory. Therefore, the number of dampers can be reduced compared to the oil damper design. However, when the design for tuned the 1st mode is performed on a high-rise building, there is a problem that the response control effect of the higher mode is almost none. Therefore, it is necessary to consider the design of higher mode control for high-rise buildings. Based on this situation, the purpose of this paper is to establish a more efficient seismic control structure. This paper proposes the tuned dynamic mass system using viscoelastic damper and its design method, and verifies the effectiveness of higher modes control from vibration testing of a multi-DOF system model.

Keywords: response control, dynamic mass (D.M.), tuned dynamic mass system, viscoelastic damper, vibration testing, amplification factor, higher modes control

1. Introduction

In many cases, the response control of buildings such as winds or earthquakes mainly adding stiffness elements or adding damping elements to absorb vibration energy. On the other hand, in recent years, a device that generates an inertial resistance according to the relative acceleration between two mass points has been proposed, and a response control design using an apparent “mass elements” is possible.

In this paper, such the device is called dynamic mass (D.M.) [1]. In the past research, there are two types of design methods using the D.M.: “Mode control” and “Tuned mode control”.

The mode control method is to make the participation vector of any mode except the 1st mode zero by manipulating the mass term of the vibration equation by the D.M. [2]. We call it “Complete mode control”. However, the amount of D.M. required to perform complete mode control is very large, “Pseudo-mode control” [3] has been proposed as an improvement.



The tuned mode control method is a vibration control device similar to TMD, and many studies have been conducted. When a D.M. and a spring element are connected in series and installed in a structure, a new vibration system (D.M. mode) can be constructed. The target mode can be got a large damping factor by adding a damping element to the new vibration system based on the fixed point theory ([4], [5]).

In previous studies ([6], [7]), a simple design method using the tuned dynamic mass system that a D.M. and a viscous damping element are arranged in parallel, and a spring element is arranged in series of they has been proposed. The optimum tuning conditions and optimum damping factor of the tuned dynamic mass system can be expressed by the relational expression of natural period. In this paper, we call it “MC-K type” for short. The MC-K type has a greater damping effect than the design of the oil damper because it gives a large damping factor to the target mode. However, when the optimum design for tuned the 1st mode is performed on a high-rise building, there is a problem that the response control effect of the higher mode is almost none. Therefore, it is necessary to consider higher mode design for high-rise buildings ([8], [14]).

On the other hand, in studies by Chen et al., Isoda et al., Saitoh, Lazar et al. ([9], [10], [11], [12]), an analysis model was proposed in which a spring element and a viscous damping element are arranged in parallel, and a D.M. is arranged in series of they. In this paper, we call it viscous damping and spring stiffness (M-CK) parallel type tuned dynamic mass system, or “M-CK type” for short.

For example, the study of Lazar et al., they tuned the 1st mode of a 3-DOF system using the TMD design formula [12] and a parametric study of the spring stiffness and the damping coefficient. In that example, it shows that the absolute displacement amplification factor of the 2nd and 3rd order modes is reduced by numerical analysis.

In this paper, we propose an optimum design formula and a simple design method of the M-CK type using the relational expression of natural period. It is also shown that it can be applied to a multi-DOF system model. We also propose the M-CK type using viscoelastic damper. The purpose of this study is to verify the effectiveness of the KC-type from the vibration testing of a multi-DOF system model, and to establish a more efficient seismic control structure.

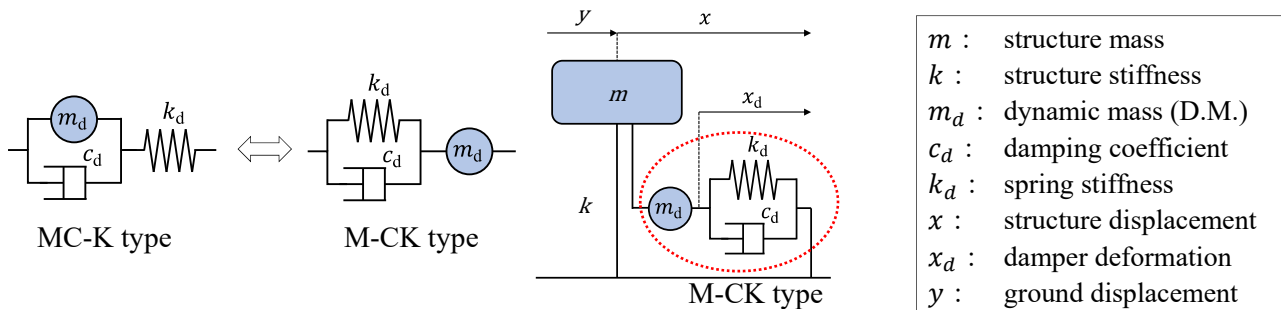


Fig. 1 – 1-DOF system model of the M-CK type

2. The optimum design formula of the M-CK type

In this chapter, we derive the “optimum tuning formula” and the “optimum damping formula” of the M-CK type shown in Fig. 1. First, the natural period T_∞ is $2\pi\sqrt{(m + m_d)/k}$ when the damping coefficient c_d is ∞ . We set the mass ratio γ_m to be m_d/m and the natural period T_0 during the Non-seismic (without the KC-type) is $2\pi\sqrt{m/k}$. If the relationship with the above T_0 and T_∞ was arranged, the mass ratio γ_m becomes a relational expression of the period as shown in Eq. (1).

$$\gamma_m = \left(\frac{T_\infty}{T_0}\right)^2 - 1 \quad (1)$$

The dynamic balance formula of the M-CK type is as shown in Eq. (2) and Eq. (3).

$$(m + m_d)\ddot{x} - m_d\ddot{x}_d + kx = -m\ddot{y} \quad (2)$$

$$-m_d\ddot{x} + m_d\ddot{x}_d + c_d\dot{x}_d + k_d x_d = 0 \quad (3)$$



Here, we set the stiffness ratio γ_k to be k_d/k . In Eq. (2) and Eq. (3), let harmonic vibration to be $x = X e^{i\omega t}$, $x_d = X_d e^{i\omega t}$, $\ddot{y} = -\omega^2 Y e^{i(\omega t + \phi)}$, and the equation of the intersection (fixed point) [7] of the relative displacement amplification factor of $c_d = 0$ and $c_d = \infty$ are obtained as shown in Eq. (4). And we set λ to be ω/ω_0 , ω_0 is the natural frequency during the Non-seismic.

$$(\gamma_m + 2)\lambda^4 - 2\left(1 + \gamma_k + \frac{\gamma_k}{\gamma_m}\right)\lambda^2 + 2\frac{\gamma_k}{\gamma_m} = 0 \quad (4)$$

If the solution of Eq. (4) are set as λ_P^2 and λ_Q^2 , the solution of the equation can be expressed by Eq. (5).

$$\lambda_P^2 = \frac{2\left(1 + \gamma_k + \frac{\gamma_k}{\gamma_m}\right) + \sqrt{\left[2\left(1 + \gamma_k + \frac{\gamma_k}{\gamma_m}\right)\right]^2 - 8(\gamma_m + 2)\frac{\gamma_k}{\gamma_m}}}{2(\gamma_m + 2)}, \quad \lambda_Q^2 = \frac{2\left(1 + \gamma_k + \frac{\gamma_k}{\gamma_m}\right) - \sqrt{\left[2\left(1 + \gamma_k + \frac{\gamma_k}{\gamma_m}\right)\right]^2 - 8(\gamma_m + 2)\frac{\gamma_k}{\gamma_m}}}{2(\gamma_m + 2)} \quad (5)$$

The condition that the amplification factor of fixed points P and Q based on the fixed point theory [7] are equal is Eq. (6).

$$\gamma_m + 1 = \gamma_m/\gamma_k \quad (6)$$

If the solution of the characteristic equation when $c_d = 0$ is set to $\lambda_{0,1}^2$, $\lambda_{0,DM}^2$, the relationship of Eq.(7) can be expressed.

$$\lambda_{0,1}^2 \cdot \lambda_{0,DM}^2 = \gamma_k/\gamma_m \quad (7)$$

Substituting Eq. (1) and Eq. (6) into Eq. (7), the optimum tuning design formula of Eq. (8) can be derived. $T_{0,1}$, $T_{0,DM}$ are periods of the 1st mode and the D.M. mode, and the D.M. mode is a vibration mode by the M-CK type. The tuned dynamic mass system enables target mode tuning by the effect of separating one vibration system into two vibration systems during the Non-seismic.

$$T_\infty = \frac{T_{0,1} \cdot T_{0,DM}}{T_0} \quad (8)$$

The amplification factor of fixed points P and Q based on the fixed point theory can be expressed as $\sqrt{2/[\gamma_m(\gamma_m + 1)]}$. If the amplification factor is set to $1/(2h_{opt})$ [7], the optimum damping formula of Eq. (9) can be obtained.

$$h_{opt} \cong 0.5 \sqrt{\frac{\gamma_m(\gamma_m + 1)}{2}} \quad (9)$$

Here, we show an example of 1-DOF system model. If the parameters of the analysis model that $m = 100$ (ton), $k = 1,000$ (kN/m), and $m_d = 10$ (ton), the natural period $T_0 = 1.987$ s and $T_\infty = 2.084$ s. Substituting the mass ratio $\gamma_m = 0.1$ into the Eq. (9) results in $h_{opt} = 0.117$.

Next, when k_d is determined by complex eigenvalue analysis so as to satisfy the optimum tuning design formula of Eq. (8), $k_d = 90.9$ (kN/m). When c_d is obtained by complex eigenvalue analysis so as to satisfy $h_{DM} \cong h_{opt}$, $c_d = 11.4$ (kN·s/m). Table 1 shows the results of the complex eigenvalues. It can be confirmed that the setting of the parameters of the analysis model satisfies the optimum tuning design formula of Eq. (8) and the optimum damping factor of Eq. (9). Fig. 2(a) shows participation functions image [15]. Here, when the imaginary number has a positive value is the 1st mode, and when the imaginary number is a negative value is the D.M. mode, it can be confirmed that the phases of the 1st mode and the D.M. mode are shifted by about $\pi/2$. Fig. 2(b) shows amplification factors (relative displacement) of 1-DOF system model example. It can be confirmed that the optimum tuning in which the heights of the fixed points P and Q on amplification factors are equal and the optimum damping in which the amplification factor is optimized.

Table 1 – Complex eigenvalue analysis results of 1-DOF system model ($c_d = 0$)

Mode	Period(s)	remarks
1st	2.377	Eq. (8) $T_\infty = \frac{T_{0,1} T_{0,DM}}{T_0} = \frac{2.377 \times 1.742}{1.987} = 2.084$
D.M.	1.742	



Table 2 – Complex eigenvalue analysis results of 1-DOF system model (Excluding internal damping)

Mode	Period(s)	Damping factor h	remarks
1st	2.300	0.079	Eq. (9) $h_{DM} = h_{opt} \cong 0.5 \sqrt{\frac{\gamma_m(\gamma_m+1)}{2}} = 0.117$
D.M.	1.800	0.117	

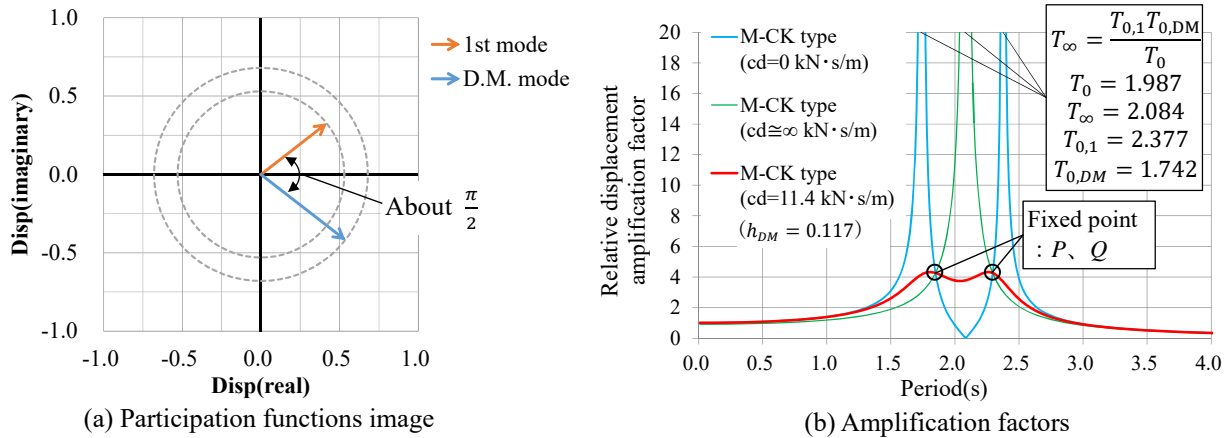


Fig. 2 – Participation functions image and amplification factors of 1-DOF system model

3. Design examples of a multi-DOF system model

In this chapter, we verify the damping effect of the MC-K type and the M-CK type using an 8-story shear model. The analysis model assumes a high-rise building, and the natural period of the 1st mode is about 3 seconds. Fig. 3 shows the analysis models, and Tables 3 and 4 show the specifications and natural periods during the Non-seismic. The MC-K type and the M-CK type are placed only in the 1st layer, and the target optimum damping factor h_{opt} is set to 0.10.

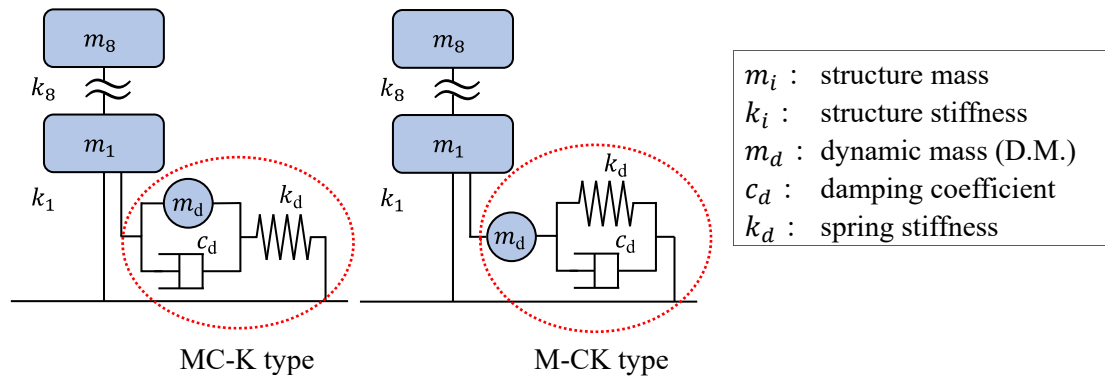


Fig. 3 – Analysis models

Table 3 – Specifications of the 8-story shear model

FL	Mass (ton)	Stiffness (kN/m)	FL	Mass (ton)	Stiffness (kN/m)
8	1.1	79.5	4	1.0	127.1
7	1.0	91.2	3	1.0	136.8
6	1.0	105.5	2	1.0	145.4
5	1.0	113.0	1	1.0	157.3

Table 4 – Natural periods of the Non-seismic

Mode	Period(s)	Mode	Period(s)
1st	3.000	5th	0.407
2nd	1.090	6th	0.351
3rd	0.674	7th	0.314
4th	0.497	8th	0.280



The parameters of the MC-K type can be calculated by a simple design method of the tuned dynamic mass system ([6], [7]). In this paper, the design procedure of MC-K type is shown in (1) to (4) below.

- (1) The target optimum damping factor is set as $h_{opt} = 0.10$, and the target auxiliary stiffness factor κ_k is obtained from the optimum damping formula. Here, the optimum damping formula $h_{opt} \cong 0.5\sqrt{\kappa_k/(2 + \kappa_k)}$, and $\kappa_k = (T_0/T_\infty)^2 - 1$.
- (2) According to complex eigenvalue analysis, k_d is determined by satisfying T_∞ with $c_d = \infty$.
- (3) According to complex eigenvalue analysis, m_d is determined by satisfying the optimum tuning formula $T_\infty = \sqrt{T_{0,1}T_{0,DM}}$ with $c_d = 0$.
- (4) According complex eigenvalue analysis, the value of c_d is determined so that the optimum damping factors h_1 and h_{DM} of the 1st mode and the D.M. mode become about 0.10.

An example of a simple design method for the M-CK type is shown in (1) to (4) below.

- (1) The target optimum damping factor is set as $h_{opt} = 0.10$, and the target mass ratio γ_m is obtained from the optimal damping equation of Eq. (9). T_∞ can be calculated from the mass ratio γ_m in Eq. (1).
- (2) According to complex eigenvalue analysis, m_d is determined by satisfying T_∞ with $c_d = \infty$.
- (3) According to complex eigenvalue analysis, k_d is determined by satisfying the optimum tuning formula of Eq. (7) with $c_d = 0$.
- (4) According complex eigenvalue analysis, the value of c_d is determined so that the damping factor h_{DM} of the D.M. mode is about 0.10.

Table 5 shows analytical model target values and optimum parameters, Table 6 and 7 show complex eigenvalue analysis results with optimum parameters, and Fig. 4 shows participation functions image. From the participation functions image, it can be confirmed that the imaginary part of the image diagram of the participation functions in the D.M. mode is a negative value, as in the examination example of 1-DOF system model.

From the complex eigenvalue results, it can be confirmed that the M-CK type is given damping factors to higher modes than the MC-K type. This is because vibration control devices of the KC-type have the effect of giving a pseudo stiffness proportional damping by arranging the spring and the viscous damping in parallel. In a multi-DOF system model using the M-CK type, viscous damping can be applied not only to the tuned 1st mode but also to higher modes.

Table 5 – Analysis model target values and optimum parameters

Model	Target h_{opt}	Target κ_k or γ_m	T_0 (s)	T_∞ (s)	m_d (ton)	c_d (kN·s/m)	k_d (kN/m)
MC-K type	0.10	0.083 (κ_k)	3.000	2.882	13.8	12.4	117.0
M-CK type	0.10	0.074 (γ_m)	3.000	3.110	11.0	12.7	59.4

Table 6 – Complex eigenvalue analysis results with optimum m_d and k_d ($c_d = 0$)

MC-K type			M-CK type		
Mode	Period(s)	remarks	Mode	Period(s)	remarks
1st	3.322	$T_\infty = \sqrt{T_{0,1}T_{0,DM}}$	1st	3.436	$T_\infty = \frac{T_{0,1}T_{0,DM}}{T_0}$
D.M.	2.498		D.M.	2.717	

Table 7 – Complex eigenvalue analysis results with optimum parameters (Excluding internal damping)

MC-K type			M-CK type		
Mode	Period(s)	h	Mode	Period(s)	h
1st	3.190	0.100	1st	3.304	0.066
D.M.	2.601	0.100	D.M.	2.768	0.100
2nd	1.039	0.001	2nd	1.052	0.031
3rd	0.647	0.000	3rd	0.647	0.037
4th	0.479	0.000	4th	0.473	0.041

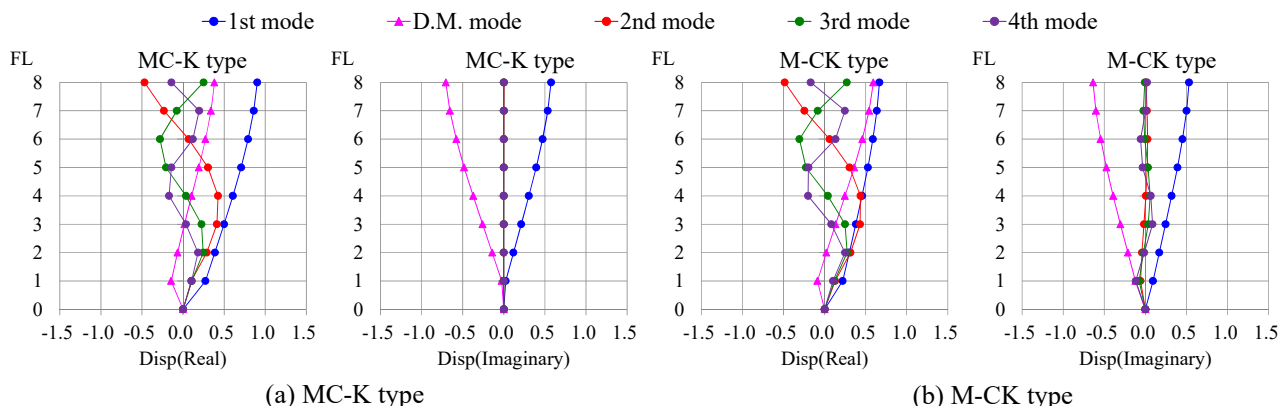


Fig. 4 – Participation functions image of seismic control structure

Fig. 5 shows the amplification factors of analysis models. The internal damping all of analysis models are Rayleigh damping ($h_1 = h_2 = 0.02$). In Fig. 5(a) and Fig. 5(b), the optimum tuning and the optimum damping of the MC-K type and the M-CK type are confirmed. In Fig. 5(c), the comparison of amplification factor of the 1st mode is reduced by about 80% in both seismic control models against the Non-seismic. On the other hand, the amplification factor of the 2nd and 3rd modes cannot be reduced with the MC-type, but is reduced by about 50% with the M-CK type, and the higher modes control can be confirmed.

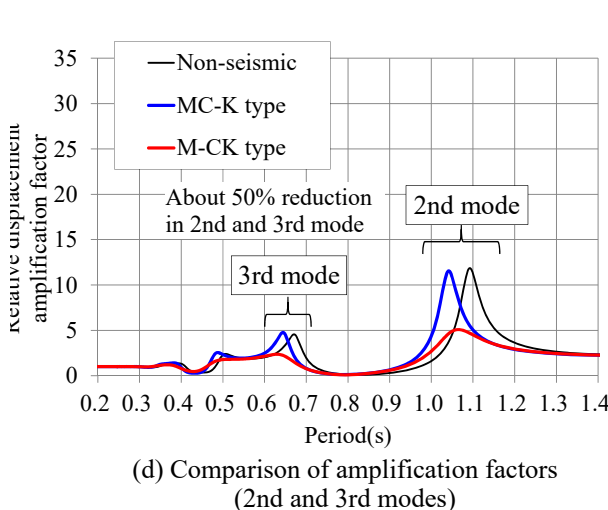
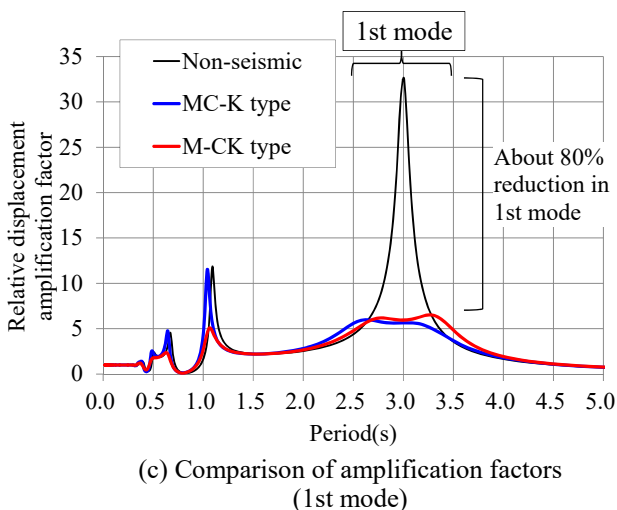
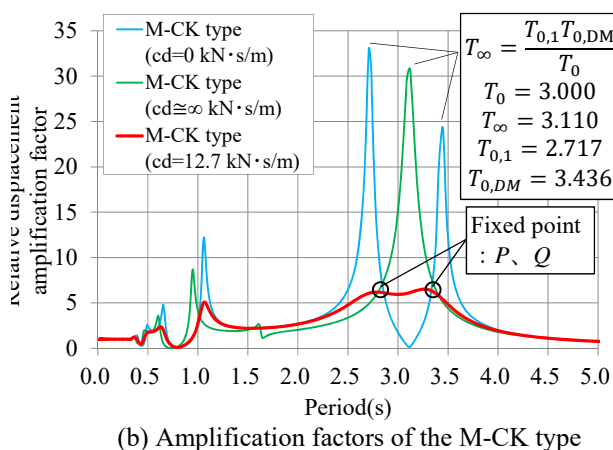
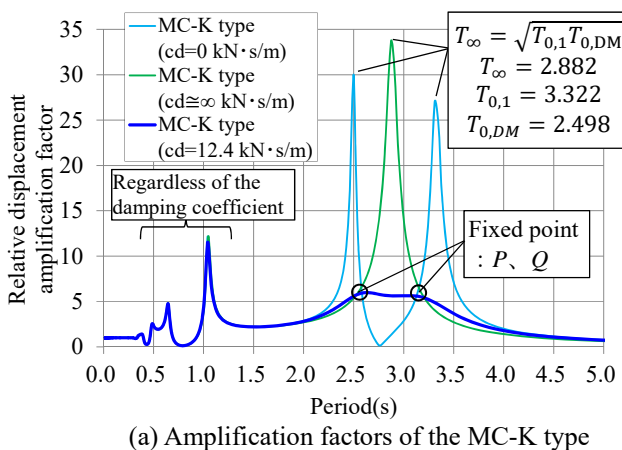


Fig. 5 – Amplification factors of analysis models (8th layer)



4. The outline of vibration testing models

In this paper, the effectiveness of higher modes control by the M-CK type was tested using an 8-story shear model. Fig. 6 shows elevation of the 8-story shear model and seismic control devices layout. The model is assumed to be a 30-story high-rise building, and the natural period of the 1st mode is set to about 3 seconds. The weight of each layer is about 10kN, and coil springs are disposed between the layers. In addition, we use linear guides for the model, so that it only affects shear deformation. Tables 3 and 4 show the specifications and natural periods during the Non-seismic.

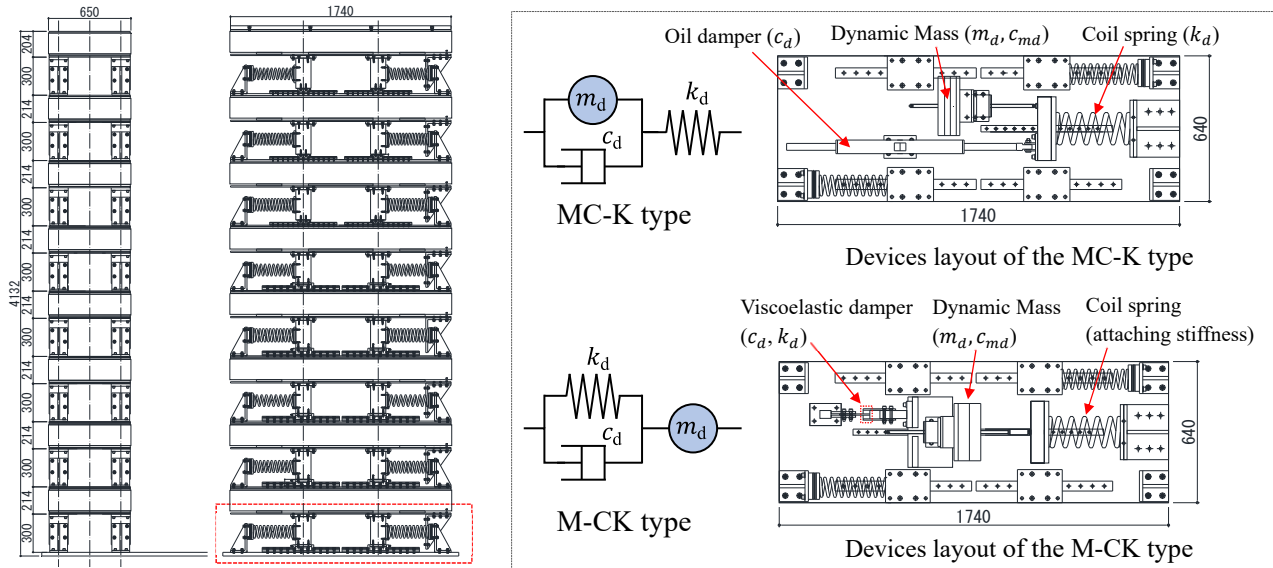


Fig. 6 – Elevation of the 8-story shear model and seismic control devices layout

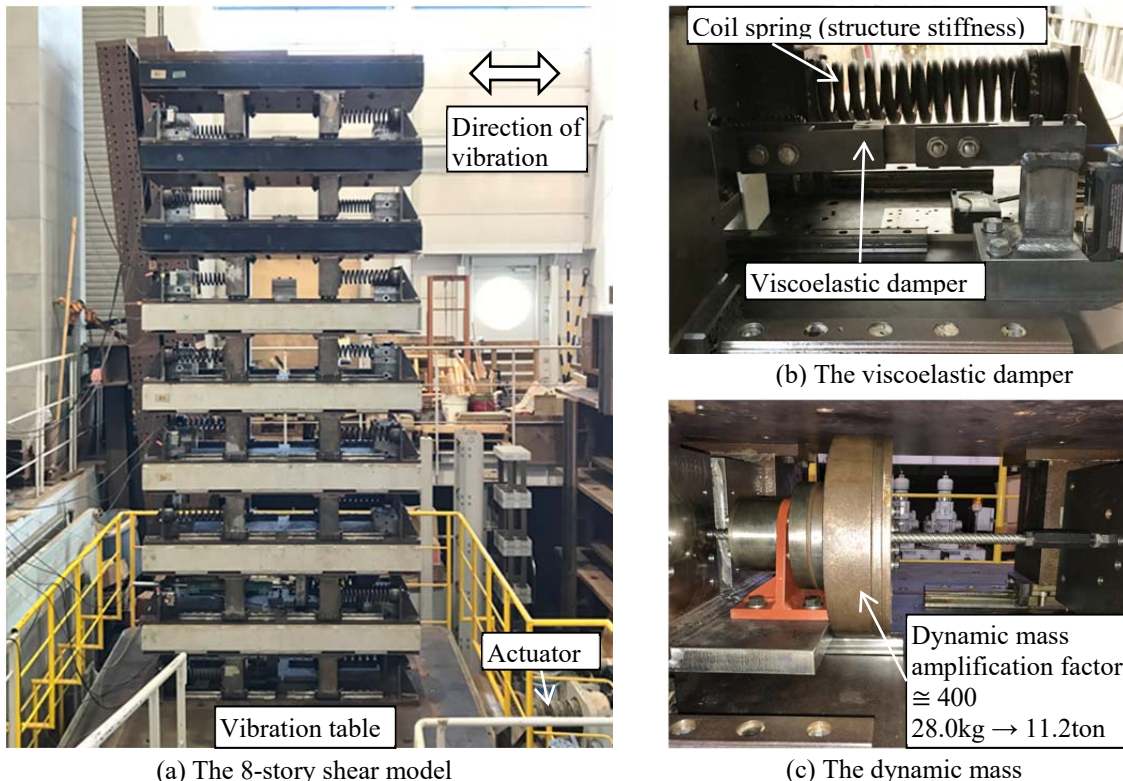


Fig. 7 – Appearance photos of the 8-story shear model and devices of the M-CK type



In order to compare the response performance of different tuned dynamic mass systems, we used the MC-K type and the M-CK type, and installed the vibration control device only in the 1st layer. In the MC-K type, D.M. and oil damper are arranged in parallel, and in the M-CK type, viscoelastic damper and D.M. are arranged in series. In addition, for convenience in mounting the M-CK type vibration damping device, the M-CK type coil spring is installed in series with the M-CK type.

The viscoelastic damper of the M-CK type has two characteristics: stiffness spring and viscous damping, so the damper is expected to be compact. Fig. 7 shows appearance photos of 8-story shear model and devices of the M-CK type. Table 8 shows optimum parameters, and Table 9 shows design parameters. Design parameters differ from the optimum parameters due to restrictions on the manufacture of dampers for each model. Table 10 shows complex eigenvalue analysis results, and Fig. 8 shows amplification factor of seismic control models. The amplification factor of the tuning mode (1st order) of the design parameters is inferior to the optimum parameters due to the manufacturing effect, but it can be confirmed that the damping factors are given to the higher modes in the M-CK type.

Table 8 – Optimum parameters of seismic control devices

Model	m_d (ton)	c_d (kN·s/m)	k_d (kN/m)	remarks
MC-K type	18.8	21.2	248.6	$k_d = 248.6(\text{kN/m})$, $\kappa_k = 0.124$, $h_{opt} = 0.121$
M-CK type	11.2	13.2	61.0	$m_d = 11.2(\text{ton})$, $\gamma_m = 0.077$, $h_{DM} = 0.102$

Table 9 – Design parameters of seismic control devices

Model	Dynamic mass		c_d (kN·s/m)	k_d (kN/m)	Attaching stiffness (kN/m)
	m_d (ton)	c_{md} (kN·s/m)			
MC-K type	18.8	8.5	21.5	248.6	—
M-CK type	11.2	4.0	17.0	57.0	248.6

※ c_{md} : Equivalent damping coefficient of the dynamic mass device. (The influence of internal friction of device)

※ k_d and c_d of the viscoelastic damper [13] : Temp.25°C, Period 3.0 s, shearing strain $\gamma=1.33(20.0\text{mm})$.

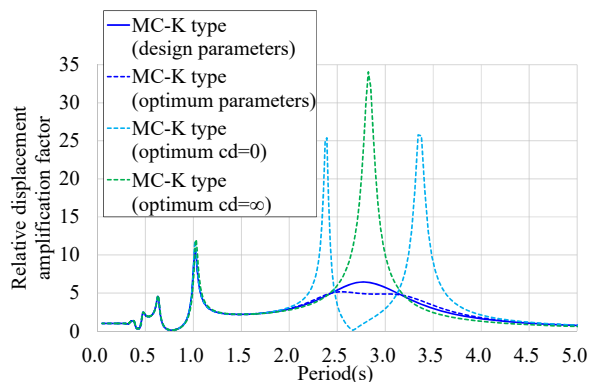
Table 10 – Complex eigenvalue analysis results of seismic control models (Excluding internal damping)

(b) Optimum parameters

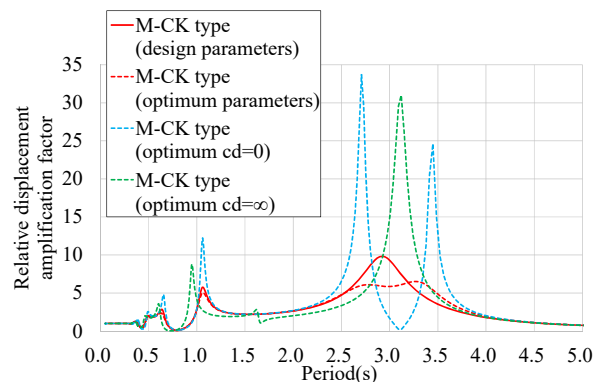
MC-K type(optimum)			M-CK type(optimum)		
Mode	Period(s)	h	Mode	Period(s)	h
1st	3.200	0.121	1st	3.306	0.065
D.M.	2.504	0.120	D.M.	2.762	0.102
2nd	1.017	0.002	2nd	1.051	0.031
3rd	0.635	0.000	3rd	0.646	0.037
4th	0.470	0.000	4th	0.472	0.041

(b) Design parameters

MC-K type(design)			M-CK type(design)		
Mode	Period(s)	h	Mode	Period(s)	h
1st	2.851	0.175	1st	3.379	0.226
D.M.	2.810	0.170	D.M.	2.942	0.056
2nd	1.018	0.003	2nd	1.052	0.024
3rd	0.635	0.001	3rd	0.647	0.022
4th	0.470	0.000	4th	0.476	0.019



(a) MC-K type



(b) M-CK type

Fig. 8 – Amplification factor of seismic control analysis models (8th layer)



5. Performance verification by sine vibration testing

In this chapter, we conducted sine vibration testing to verify the damping effect of seismic control models. The relative displacement amplification factors were determined as the result of tests. The vibration table displacement, story drift of each layer, and damper deformation are measured by laser displacement meters, and the acceleration of each layer is measured by accelerometers. In addition, we install thermocouple meters in the viscoelastic damper and measure the temperature.

The viscoelastic damper of the M-CK type has various dependencies such as temperature dependency. Therefore, in order to reduce these effects, we conducted sine vibration testing for an 8-story shear model under the condition of maintaining the temperature of 25°C and the shearing strain $\gamma = 1.33$ (20.0 mm).

Condition 1: In order to reduce the effect of the temperature dependence, pre-vibration is performed before the viscoelastic damper temperature reaches about 25°C.

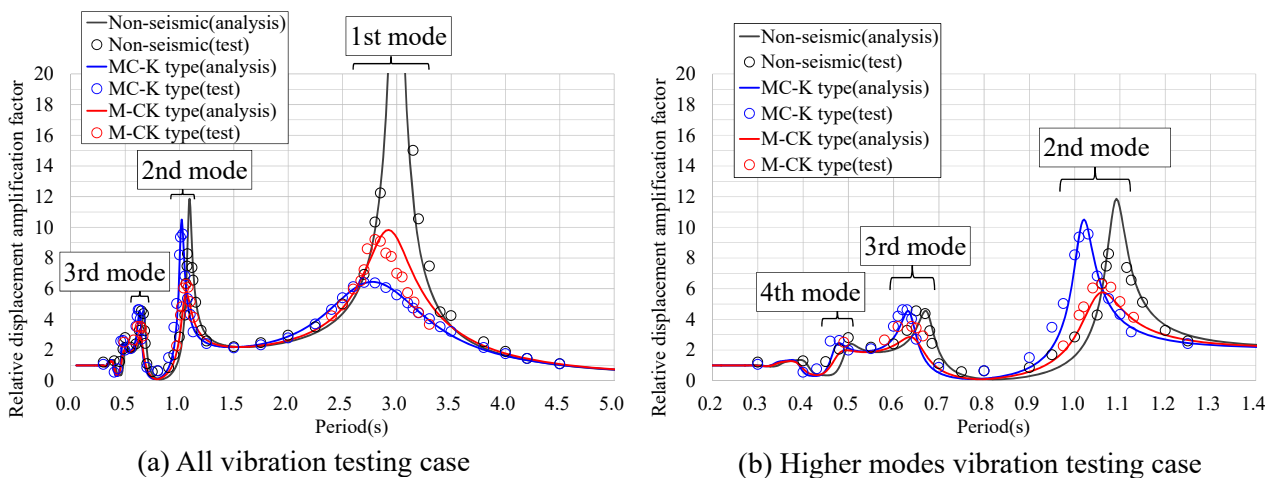
Condition 2: In order to reduce the effect of the amplitude dependency, the input amplitude on the vibration table is adjusted so that the shear strain γ is about 1.33 (20.0mm).

The range of the vibration table excitation cycle is 0.30 seconds to 4.50 seconds. As an evaluation, we calculate the relative displacement amplification factor of the 8th layer displacement with respect to the vibration table displacement. In addition, we compare the amplification factor of the test values and the analysis values.

Fig. 9 shows the relative displacement amplification factors of the 8th layer of each model. The black marker is the Non-seismic, the blue marker is the MC-K type, and the red marker is the M-CK type. The solid line represents the analysis values of design, and the marker represents the test values. It can be confirmed that the test values and the analysis values correspond roughly.

On the other hand, the M-CK type has some variation in the 1st mode. The reason is considered to be that the spring stiffness of the viscoelastic damper is not always constant in the test values due to frequency and repetition dependency. Compared to the amplification factor of the Non-seismic, it can be confirmed that the amplification factor of the 1st mode is reduced for both the MC-K type and the M-CK type.

In Fig 9, it can be confirmed that the amplification factor of the 2nd and 3rd modes is large in the MC-K type, and the amplification factor of the 2nd and 3rd modes is reduced in the M-CK type. Based on the above results, the effectiveness and robustness of the tuned dynamic system (M-CK type) using viscoelastic damper for higher modes control was verified regardless of the frequency and repetition dependency of the viscoelastic damper.



※The internal damping all of analysis models are Rayleigh damping ($h_1 = h_2 = 0.02$).

Fig. 9 – Amplification factor of vibration testing (8th layer)



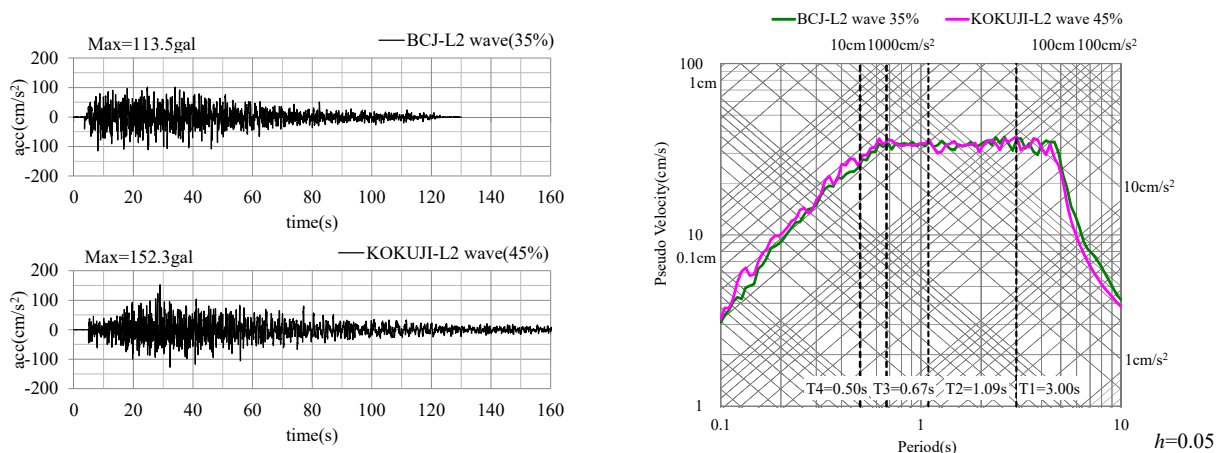
6. Performance verification by simulated ground motion vibration testing

Table 11 shows simulated ground motions of the vibration testing. (1) BCJ-L2 wave is simulated wave by the Building Center of Japan, and (2) KOKUJI-L2 wave is a simulated wave created by the notification of the Building Standard Law of Japan. Fig. 10 shows the simulated ground motion waveforms and the response spectrum. In addition, we adjust the input amplitude of the simulated ground motions so that the maximum response displacement of the Non-seismic does not exceed 30cm.

Fig. 11 shows experimental results for simulated ground motions. It can be confirmed that the maximum response displacement of the MC-K type and the M-CK type are reduced compared to the Non-seismic. It can also be confirmed that the maximum response acceleration of the M-CK type is reduced compared to the Non-seismic and the MC-K type. In simulated ground motion vibration testing, the effectiveness of the tuned dynamic mass system using viscoelastic damper for higher modes control was verified.

Table 11 – Simulated ground motions

Simulated ground motion	Peak ground acceleration(cm/s ²)	Peak ground velocity(cm/s)	Time(s)
(1)BCJ-L2 wave 35%	113.5	16.8	120
(2)KOKUJI-L2 wave 45%	152.3	15.0	160



※ Simulated ground motions are low-frequency filtered to prevent excessive displacement of the vibration table.

Fig. 10 – Simulated ground motion waveforms and response spectrum

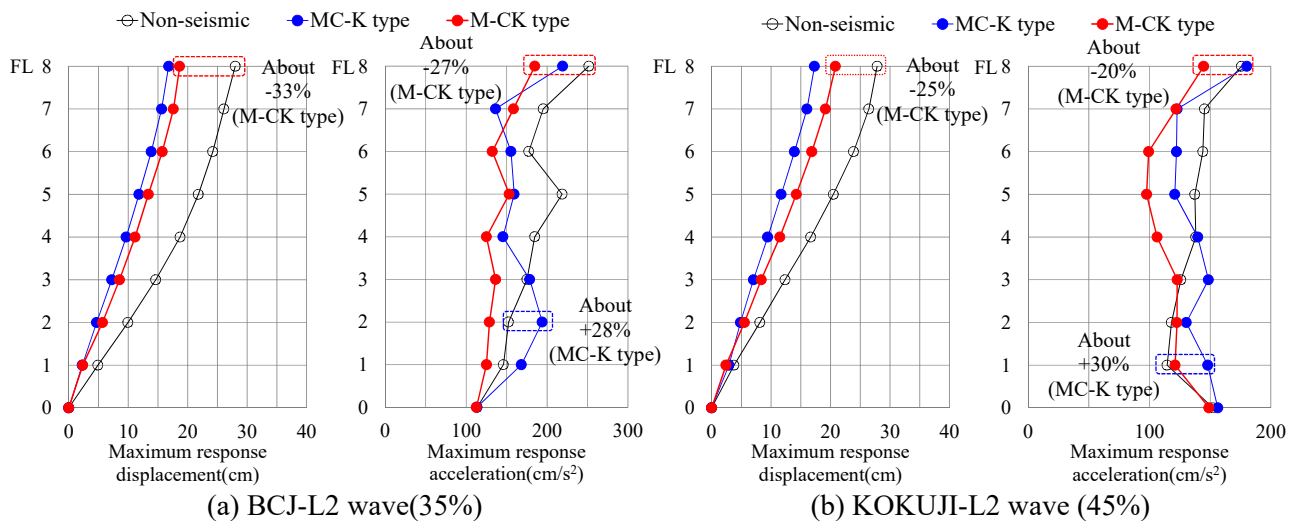


Fig. 11 – Experimental results for simulated ground motions



7. Conclusion

In this paper, we theoretically derived “the optimum tuning formula” and “the optimum damping formula” for the M-CK type setting method. It was confirmed that the optimum design formula can be applied to a multi-DOF system by expressing it with the relational expression of natural period.

In the example using the M-CK type, according to the complex eigenvalue analysis results, the damping factor was simultaneously given to not only the tuned 1st mode but also the higher modes. It can also be confirmed from the amplification factor that the response is reduced. We also gave an overview of the vibration testing of the 8-story shear model and the results. The experimental results verified the effectiveness of the tuned dynamic mass system (M-CK type) using viscoelastic damper and showed the possibility of a more efficient seismic control structure.

8. References

- [1] Ishimaru, S.: Seismic design method (Invitation to Dynamic Design), KENCHIKUGIJYUTU, 2008 (in Japanese).
- [2] Furuhashi, T. and Ishimaru, S.: Response Control of Multi-Degree System by Inertial Mass (Study on response control by inertial mass No.2), Journal of Structural and Construction Engineering, No. 601, 83–90, 2006 (in Japanese).
- [3] Ishimaru, S., Hata, I., and Furuhashi, T.: A simple design methods for tuned dynamic mass systems by Pseudo Mode Control, Journal of Structural and Construction Engineering, Vol. 76, No. 661, 509–517, 2011 (in Japanese).
- [4] Saito, K. Kurita, S. Inoue, N.: Optimum Response Control of 1-Dof System Using Linear Viscous Damper with Inertial Mass And Its Kelvin-Type Modeling, Journal of Structural Engineering, Vol.53B, 53–66, 2007 (in Japanese).
- [5] Inoue, N. and Ikago, K.: Building displacement control design (Seismic isolation and long-period building design methods for earthquakes), MARUZEN , 2012 (in Japanese).
- [6] Ishimaru, S., Mikami, J., Hata, I., and Furuhashi, T.: A simple design methods for tuned dynamic mass systems, Journal of Structural and Construction Engineering, Vol. 75, No. 652, 1105–1112, 2010 (in Japanese).
- [7] Ishimaru, S., Hata, I., Mikami, J., and Kimizuka, M.: A simple design method for tuned dynamic mass systems on the basis of auxiliary stiffness factor, Journal of Structural and Construction Engineering, Vol. 75, No. 654, 1455–1464, 2010 (in Japanese).
- [8] Kuo, C., Ishimaru, S., Furuhashi, T., and Hata, I.: A Design Method for Structures with Tuned Dynamic Mass Systems (Response control design of next-generation super high-rise structures against long period waves and pulse wave earthquake ground motions), Journal of Structural and Construction Engineering, Vol. 78, No. 686, 693–702, 2013 (in Japanese).
- [9] Chen, M. et al.: The missing mechanical circuit element, Circuits and Systems Magazine, IEEE, 9(1); 10–26, 2009.
- [10] Isoda, K., Hanzawa, T., and Tamura, K.: A Study on Response Characteristics of A SDOF Model with Rotating Inertia Mass Dampers, Journal of Structural and Construction Engineering, Vol. 74, No. 642, 1469–1476, 2009 (in Japanese).
- [11] Saitoh, M.: On the performance of gyro-mass devices for displacement mitigation in base isolation systems, Structural Control and Health Monitoring, Vol. 19, No. 2, 246–259, 2012.
- [12] Lazar, I.F., Neild, S.A., Wagg, D.J.: Using an inerter-based device for structural vibration suppression, Earthquake Engineering and Structural Dynamics, 43; 1129–1147, 2014.
- [13] Kaneshiro, Y. et al.: Stud-type viscoelastic damper using high damping rubber (Part.1 Performance verification by full-scale test), Architectural Institute of Japan, 595–596, 2017 (in Japanese).
- [14] Miyajima, Y., Hata, I., Mashimo, M., Ogihara M., and Ishida, T.: Response Control Systems by Tuned Dynamic Mass System for a 200-meter-tall tower-supported steel stack structure, Proceedings of the 16th World Conference on Earthquake Engineering, paper ID 1363, 2017.
- [15] Ishimaru, S.: Introduction of Seismic Response Control Design, SHOKOKUSHA, 2004 (in Japanese).